BLAST Observations of the Low-Mass Star Forming Region IC 5146

Kevin France[1], BLAST Collaboration[2]

ABSTRACT

IC 5146 is a star forming region in Cygnus, consisting of a young massive star cluster and lower mass regions that are just beginning to form stars. We present sub-mm observations of the low-mass northern streamer region of IC 5146. The dense cores in this region are thought to be pre-stellar and have been studied previously by SCUBA and molecular line observations. The new sub-mm observations were carried out during the 2005 flight of the Balloon-borne Large-Aperture Sub-millimeter Telescope (BLAST). The data are broadband images centered on 250, 350, and 500 μm. We combine the BLAST images with archival IRAS and Spitzer-MIPS observations to determine the spectral energy distributions (SEDs) of several point-like and diffuse sources in IC 5146. The SEDs reveal dust temperatures of roughly $\sim$14 K for both diffuse filaments and regions containing IRAS point sources and/or known protostars. We also present evidence for variations in the spatial distribution of grain temperatures in the region. These observations will allow us to constrain simple models of pre-stellar clouds and will support the upcoming Herschel - SPIRE Gould Belt Survey.

Subject headings: infrared: ISM — ISM: dust, extinction — ISM: structure

1. Introduction

IC 5146 is a molecular cloud complex in Cygnus. It is composed of an open cluster of surrounded by bright optical nebulosity (The Cocoon Nebula) and a region of embedded lower mass star-formation known as the IC 5146 Northern Streamer or IC 5146 Dark Cloud

[1]Center for Astrophysics and Space Astronomy, University of Colorado, Boulder, CO 80309

[2]http://blastexperiment.info/

(Bergin et al. 2001). The Northern Streamer region (d = 460 pc; Lada et al. 1999) is a highly reddened region of roughly a dozen protostars inferred from IRAS point sources or CO outflows (Dobashi et al. 2001 and references therein), as well as a dense central ridge thought to contain several pre-stellar cores (Kramer et al. 2003).

This proceeding focuses on 5 sub-regions of the IC 5146 Northern Streamer. Region A covers the bright FU Orionis object V1735 Cyg. This Class I protostar (0.42 $M_\odot$) is an extended object, associated with a near-IR reflection nebula (Connelley et al. 2007) and a higher-mass (2.0 $M_\odot$) protostar (V1735 Cyg SM 1) that dominates the 450 and 850 μm flux from the object. Region B is the central ridge, where the regions of highest visual extinction ($A_V \geq 12$ mag; Lada et al. 1999) show evidence for CO depletion as the molecules freeze out onto grain surfaces (Kramer et al. 1999; Bergin et al. 2001). Visual extinction maps of Region B have also been compared to SCUBA sub-mm observations in order to study the variation of the dust emissivity with dust temperature (Kramer et al. 2003).

Region C encompasses several IRAS point sources with CO outflows, evidence for protostellar activity. Region D is the isolated point source IRAS 21432+4719, the second brightest far-IR source in the region. Region E is to the south of the ridge, and is related to the LDN 1031 dark cloud. It coincident with an IRAS point source without an associated CO outflow, suggesting that it may also be in an earlier evolutionary state. However, there is evidence that the LDN1031 cloud is not physically associated with the Northern Streamer (d_{1031} = 200 pc; Maheswar & Bhatt 2006).

In this work, we present new observations of the IC 5146 Northern Streamer made by the Balloon-borne Large-Aperture Sub-mm Telescope (BLAST). BLAST is a survey instrument designed to study star-formation in both the local and distant universe. In Section 2, we briefly describe the BLAST experiment, the observations of IC 5146, and supporting data from IRAS and the MIPS instrument on the *Spitzer Space Telescope*. Section 3 discusses the data analysis and the creation of spectral energy distributions (SEDs) for Regions A – E. Finally, in Section 4, we discuss the different grain populations in the Northern Streamer region and future directions.

2. BLAST Observations and Supporting Data

BLAST is a 2-m Cassegrain telescope mounted into a gondola for balloon-borne stratospheric (altitude $\geq$ 35 km) observations. BLAST uses 270 bolometers grouped into three arrays for simultaneous observing in three sub-mm bands. The detector arrays observe in broad bands ($\Delta\lambda$ / $\lambda \approx 0.3$) at 250 μm (139 detectors), 350 μm (88 detectors), and 500 μm

(43 detectors). The nominal resolutions of the instrument are 30, 42, and 60″ at 250, 350, and 500 μm, respectively.

The northern streamer region of IC 5146 (Bergin et al. 2001) was observed by BLAST during a 100-hour flight in 2005 June. The telescope was launched from Kiruna, Sweden and was recovered in northern Canada, observing several large galactic fields (Truch et al. 2008; Chapin et al. 2008). A roughly $1^{\circ} \times 1^{\circ}$ field centered on (R.A. (J2000) = 326.5437°, Dec. (J2000) = 47.5769°) was observed in the three BLAST bands during the flight. The raw bolometer data were processed into source maps using the SANEPIC map-making algorithm (Patanchon et al. 2008). The 250, 350, and 500 μm maps of IC 5146 are shown in Figure 1. Due to a degradation of optical system focus during the 2005 flight, the maps presented in this work have a spatial resolution of 4–5′, and are sampled at 10″ pixel^{-1}.

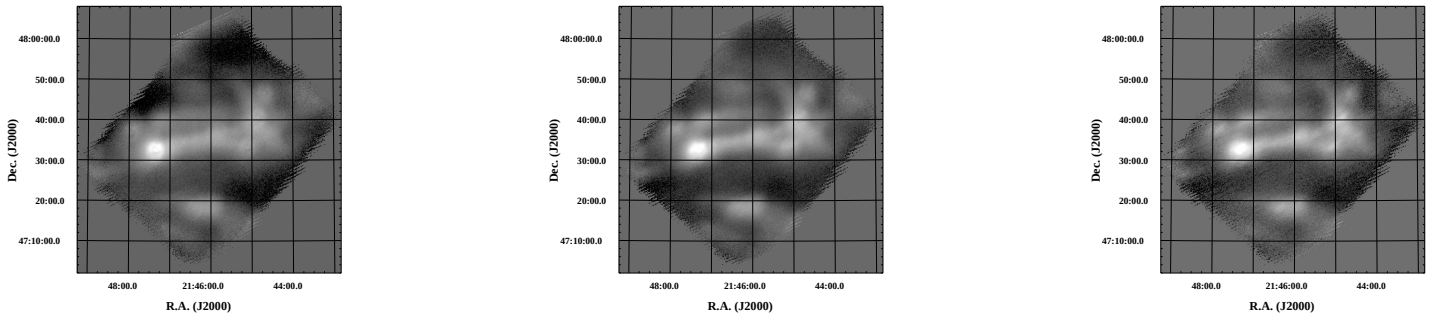

Fig. 1.— (*Left to Right*) 250, 350, and 500 μm BLAST maps of IC 5146. The bright source to the left of the images is the FU Ori star V1735 Cyg and its associated sum-mm peak SM 1.

Archival data from IRAS and *Spitzer* were acquired to complement the new BLAST maps. The reprocessed IRAS maps, IRIS, were obtained in the 60 and 100 μm bands, with a spatial resolution of $\sim 4'$ (Miville-Deschnes & Lagache 2005). We also obtained *Spitzer*-MIPS (Rieke et al. 2004) images of the IC 5146 field at 70 and 160 μm. The 70 μm data only covered a small fraction of the BLAST field, however the 160 μm map covered $\approx 50\%$ of the BLAST field, and these data were included in the analysis when available (described in the next section). IC 5146 was observed by MIPS on 2004 November 09 as part of the P00053 program (data set identifier 0012024576). The 160 μm map was obtained using the SSC Leopard archive tool, and was convolved to the BLAST resolution using a two-dimensional Gaussian kernel. The supporting *Spitzer* and IRIS maps were regridded to the BLAST pixel scale and astrometry prior to analysis.

3. Subregion Analysis and Spectral Energy Distributions

The astrometry of the BLAST maps relative to the regridded IRIS and MIPS data was compared for the brightest source in the field, V1735 Cyg. The source is extended, however the core of the region is point-like, and Gaussian fits were made in right ascension and declination in the 100, 160, and 250 μm bands. We find that the central pixels in both direction are offset no more than [ΔR.A., ΔDec.] = [1.6, 1.3] pixels. At the $10''$ pixel^{-1} plate scale, this is significantly smaller than the resolution element for each of the three instruments. Furthermore, the actual peak may be wavelength dependent, as the sub-mm peak is coincident with the SM 1 object (Sandell & Weintraub 2001) while the shorter wavelength data may receive a greater contribution from the FU Ori star itself. Suffice to say, we feel that the astrometry alignment between the data sets is sufficient for the analysis presented below.

Towards checking the absolute astrometry of the BLAST maps, we measure the SM 1 offset in the BLAST 250 μm map. Using the 450 and 850 μm SCUBA maps, Sandell & Weintraub determine that the SM 1 position is roughly $20''$ to the northeast of the FU Ori object. Comparing the peak of the 250 μm BLAST map with the FU Ori coordinates, we measure an offset of $\sim 23''$. Taking the BLAST point uncertainty to be $\leq 5''$ and the SCUBA uncertainty to be $\leq 2''$, the BLAST astrometry is consistent with previous observations.

Following the creation of self-consistent multi-wavelength maps, we calculate the SEDs of various regions in the IC 5146 field in four steps. First, we create a 'good pixel' mask by requiring that the regions have a threshold number of hits per pixel (the threshold was set to 200 hits per pixel in the 250 μm map). This masking function is then applied to all data so that no regions suffering from spurious edge effects or exceptionally low S/N influences the results. The second step involves identifying sub-regions of the data to examine. We analyzed 5 regions in the present work, encompassing cold, dusty regions both with active star-formation and those without clear evidence for protostars. These regions are outlined in the introduction and summarized in Table 1.

Due to large, variable contributions from the sky and telescope to the signal detected by stratospheric, sub-mm instruments, the large background is filtered out during the map-making process. As a result, the DC level (flux zero-point) in the BLAST maps is not known. For non-point like regions of diffuse emission with complicated spatial distributions, aperture photometry does not yield a reliable flux measurement. However, we can create relative SEDs (normalized to a fiducial wavelength, λ_o) by verifying the astrometric alignment and assuming that all of the far-IR/sub-mm bands are tracing the same material. It is the latter restriction that leads us to eliminate the IRIS 60 μm data from our fits as this band is most likely contaminated by a smaller grain population stochastically heated to higher

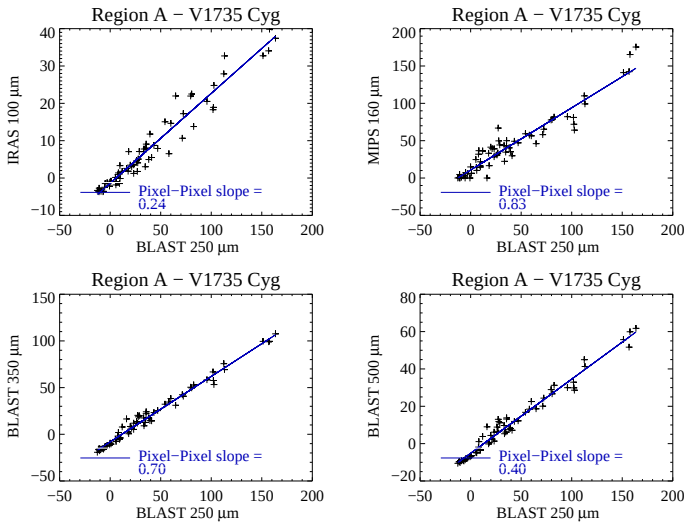

Fig. 2.— An example of the pixel-pixel comparison. The slope of the pixel-pixel relations are used to create spectral energy distributions relative to a reference wavelength (250 μm).

temperatures than the grains traced by the $\lambda \geq 100$ μm images. We rebin all of the maps to $90''$ pixel^{-1} and examine the pixel(λ_o) vs pixel(λ) correlations between the bands. A linear relation suggests that the maps are tracing a single temperature population, and in this case, the change in brightness with bandpass (wavelength) is the SED relative to the flux at λ_o. The change in flux relative to F(λ_o) is simply the slope of the correlation. An example of the pixel-pixel correlations for the 5 bands is shown in Figure 2. For the IC 5146 data, we used $\lambda_o = 250$ μm, thus our relative SEDs are normalized to F(250).

Once the relative SEDs are created, they are fit using a modified black-body curve

Table 1. Dust temperatures derived assuming the best-fit value of $\beta = 1.7$.

BLAST Region	Other Names[a]	RA (J2000) (h m s)	δ (J2000) (° ′ ″)	Subregion Dimensions (′)	T_d (K)
A	V1735 Cyg SM 1	21 47 23.6	+47 32 15	12′ × 12′	14.68 ± 1.87
B	Northern Streamer	21 46 18.4	+47 34 37	13.5′ × 24′	13.68 ± 2.04
C	IRAS 21428+4732 IRAS 21429+4726 DBY94	21 44 56.2	+47 39 26	12′ × 15′	14.14 ± 2.80
D	IRAS 21432+4719	21 45 10.2	+47 32 26	7.5′ × 7.5′	14.58 ± 2.68
E	LDN1031	21 46 14.4	+47 22 17	12′ × 13.5′	14.98 ± 1.78

[a]Refers to known sources enclosed in the BLAST extraction regions.

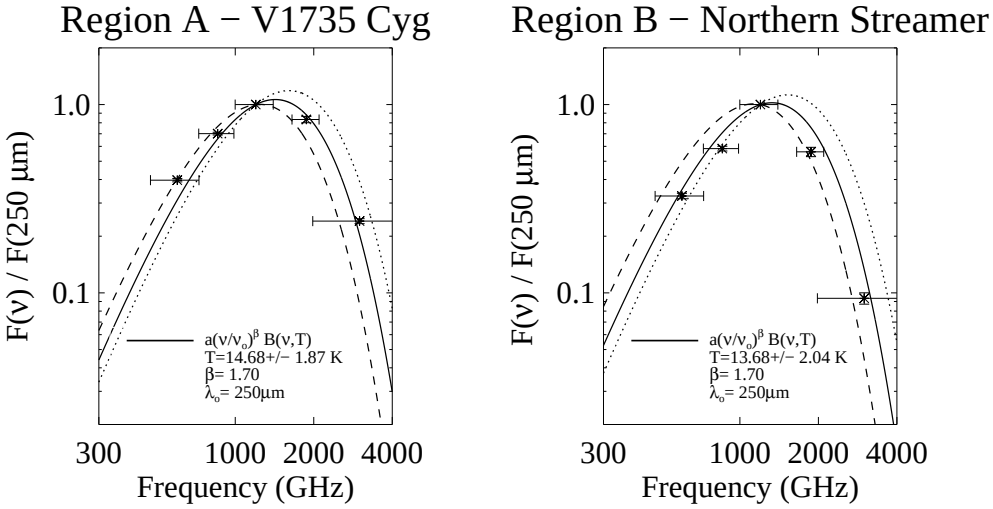

Fig. 3.— Spectral energy distributions of the FU Ori star V1735 Cyg (and the nearby sub-mm peak (Sandell & Weintraub, 2001) and the diffuse emission from the Northern Streamer. Error bars in the x-axis represent the bandpasses of each instrument. The solid line represents the best-fit temperature for $\beta = 1.7$, and the dotted and dashed lines are the SEDs for the upper and lower limits on the derived dust temperatures, respectively.

(described for BLAST observations by Chapin et al. 2008):

$$F_\nu(\beta, T_d) \propto \left(\frac{\nu}{\nu_o}\right)^\beta B_\nu(T_d) \quad (1)$$

where β is the dust emissivity index, B_ν is the Planck function, and T_d is the dust temperature. The relative SEDs are fit using an iterative χ^2 minimization. Initially, both β and T_d are allowed to vary. For all of the IC 5146 data, β converged to 1.70 ± 0.15, although the errors on the temperature fit were quite large. A second iteration was performed holding β constant at 1.7, and the resulting errors on the temperature are of order 2-3 K. Sample SEDs for Regions A and B are shown in Figure 3, and the derived temperatures for all of the IC 5146 subregions are given in Table 1. We find that the temperature is roughly 14 K in all regions in the 100 – 500 μm SEDs of IC 5146, indicating we are sampling dust in the regions where $C^{18}O$ depletion is occuring (Kramer et al. 1999).

4. Spatial Profiles

The varying contributions of large cool grains (traced by the $\lambda \geq 100$ μm SEDs) and a smaller warm grain population can be addressed by considering the IRIS 60 μm

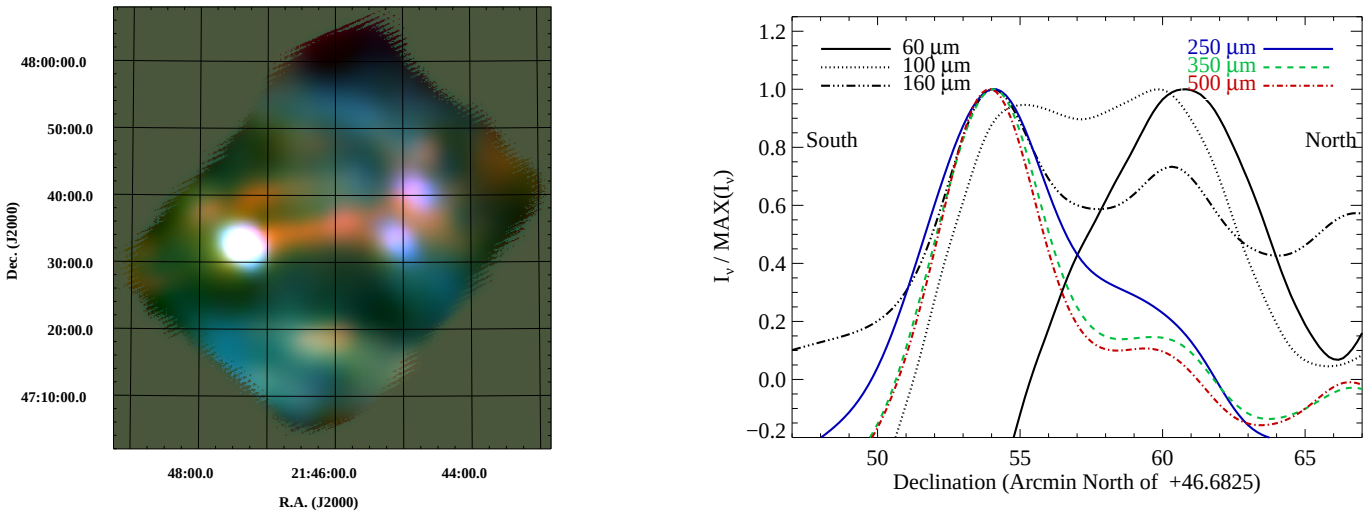

Fig. 4.— *Left*: R(350 μm), G(100 μm), B(60 μm) image of IC 5146. *Right*: Spatial profiles perpendicular to the Northern Streamer. The sub-mm data traces the cold dust in the dense, pre-star-forming northern streamer while the 60 μm emission is associated with protostars.

data in relation to the longer wavelength emission. Figure 4 (*Left*) shows a three-color image of IC 5146 in BLAST 350 μm (red), IRIS 100 μm (green), and IRIS 60 μm (blue). One immediately notices that the Northern Streamer filament is dominated by the sub-mm emission while there are isolated regions of strong 60 μm emission. The blue (60 μm) regions to the west are coincident with known IRAS point sources with CO outflows (sources 7 (IRAS 21428+4732), 8 (IRAS 21429+4726), and 9 (IRAS 21432+4719) in Dobashi et al. 2001), indicative of Class 0/Class I protostars. While there is a faint IRAS point source (IRAS 21441+4722) and CO emission in the Northern Streamer, it is thought to be a prestellar region (Kramer et al. 2003) with essentially no emission from warm grains.

A similar comparison can be made by taking spatial projections across the maps perpendicular to the Northern Streamer (that is, a cut along the declination (y-)axis). Spatial profiles were extracted from a $4'$ wide stripe running from south to north and intersecting the Northern Streamer at R.A.(J2000) = $21^h\ 46^m\ 13.9^s$ in all six imaging bands. Figure 4 (*Right*) shows the profiles from south of the Northern Streamer to the top of the map, where each profile has been normalized to 1.0 for comparison. One again sees the clear offset between the BLAST and 60 μm emission indicating a difference in the evolutionary stages of the clouds. We observe the 100 and 160 μm curves to be tracing a mix of the warm and cold phases of this region. In future work, we will examine these profiles in greater detail and use them to test simple radiative transfer models of spherical and cylindrical self-gravitating,

isothermal clouds (Fischera & Dopita 2008).

The BLAST collaboration acknowledges the support of NASA through grant numbers NAG5-12785, NAG5-13301 and NNGO-6GI11G, the Canadian Space Agency (CSA), the UK Particle Physics & Astronomy Research Council (PPARC), Canada's Natural Sciences and Engineering Research Council (NSERC), the Canada Foundation for Innovation, the Ontario Innovation Trust, the Puerto Rico Space Grant Consortium, the Fondo Istitucional para la Investigacion of the University of Puerto Rico, and the National Science Foundation Office of Polar Programs. KF acknowledges support from the Canadian Institute for Theoretical Astrophysics and thanks Joerg Fischera for helpful discussion.

REFERENCES

Lada, Alves, & Lada. 1999, ApJ, 512, 250

Kramer et al. 1999, A&A, 342, 257

Kramer et al. 2003, A&A, 399, 1073

Bergin et al. 2001, ApJ, 557, 209

Connelley, Reipurth, & Tokunga. 2007, AJ, 133, 1528

Sandell & Weintraub. 2001, ApJS, 134, 115

Maheswar & Bhatt. 2006, MNRAS, 369, 1822

Dobashi, Yonekura, & Hayashi. 2001, PASJ, 53, 811

Fischera & Dopita. 2008, ApJS, 176, 0

Pascale et al. 2008, ApJ, submitted

Patanchon et al. 2008, ApJ, accepted

Chapin et al. 2008, ApJ, accepted

Truch et al. 2008, ApJ, submitted

Rieke et al. 2004, ApJS, 154, 25

Miville-Deschnes & Lagache 2005, ApJS, 157, 302